

## Article

# Bio-Adipic Acid Production from Muconic Acid Hydrogenation on Palladium-Transition Metal (Ni and Zn) Bimetallic Catalysts

Elisa Zanella , Lorenzo Secundo, Silvio Bellomi , Alessandro Vomeri , Alberto Villa  and Carlo Pirola \* 

Dipartimento di Chimica, Università degli Studi di Milano, Via Golgi 19, 20133 Milan, Italy

\* Correspondence: carlo.pirola@unimi.it; Tel.: +39-02-5031-4283

**Abstract:** The hydrogenation of muconic acid (MA) to bio-adipic acid (AdA) is one of the green chemical processes that has attracted the most interest in recent years. Indeed, MA can be readily obtained from biomass through fermentative processes. Here, we aimed to investigate the synergic effect of electronic promotion that the addition of a second metal, even in small quantities, can have on Pd-based catalyst, known for its low stability. Ni and Zn were taken into consideration and two different catalysts (1%Pd<sub>8</sub>Ni<sub>2</sub>/HHT and 1%Pd<sub>8</sub>Zn<sub>2</sub>/HHT) were synthesized by sol immobilization method and supported on high-temperature, heat-treated carbon nanofibers (HHT-CNFs) that are known to enhance the stability of palladium. The catalysts were tested in MA hydrogenation and thoroughly characterized by TEM, ICP, and XPS analysis to unveil the effect of the second metal. To solve the solubility issue and have a starting material as similar as feasible to the post-fermentation conditions of the biomass, sodium muconate salt was chosen as a substrate for the reaction. All of the synthesized bimetallic catalysts showed a higher activity than monometallic Pd and better stability during the recycling tests, pointing out that even a small amount of these two metals can increase the catalytic properties of monometallic Pd.

**Keywords:** adipic acid; muconic acid; bimetallic catalysts; palladium; zinc; nickel; transition metals



**Citation:** Zanella, E.; Secundo, L.; Bellomi, S.; Vomeri, A.; Villa, A.; Pirola, C. Bio-Adipic Acid Production from Muconic Acid Hydrogenation on Palladium-Transition Metal (Ni and Zn) Bimetallic Catalysts. *Catalysts* **2023**, *13*, 486. <https://doi.org/10.3390/catal13030486>

Academic Editors: Victorio Cadierno and Guillermo Ahumada

Received: 30 November 2022

Revised: 22 February 2023

Accepted: 23 February 2023

Published: 27 February 2023



**Copyright:** © 2023 by the authors. Licensee MDPI, Basel, Switzerland. This article is an open access article distributed under the terms and conditions of the Creative Commons Attribution (CC BY) license (<https://creativecommons.org/licenses/by/4.0/>).

## 1. Introduction

“The continual development which satisfies the needs of the present without compromising the capacity of future generations to meet their own needs”, this is how sustainability was defined by the United Nation World Commission on Environment and Development [1]. One of the most important challenges of the 21st century is to investigate new sustainable and environmentally friendly processes, minimizing mankind’s impact on the Earth. One of the main focuses in the development of such processes is the investigation starting materials. As stated in the seventh tenet of the Green Chemistry principles, one of the main goals is the “use of renewable feedstock” [2].

In this scenario, the production of bio-adipic acid assumes a central role [3,4]. Adipic acid (AdA) is one of the most industrially significant dicarboxylics, as it is a crucial monomer in the production of plasticizers, lubricants, polyesters, and polyamides [5], in particular Nylon-6 and Nylon-6,6, of which the latter accounts for 65% of the 2.6 million tons of AdA produced annually worldwide [6]. Nowadays, AdA is commercially produced by reducing benzene to cyclohexane, which is then oxidized to a mixture of cyclohexanol and cyclohexanone, named K-A oil. This mixture is further oxidized to AdA through nitric acid. Clearly, this process is far from being environmentally sustainable, as it accounts for 10% of artificial nitrous oxide production and uses hazardous solvents, such as benzene [6].

In the last decades, a possible solution has been found in the exploitation of waste woods. Starting from lignin [7] or cellulose [8], *cis,cis*-muconic acid (MA) can be obtained through biological processes, which is subsequently catalytically hydrogenated to bio-adipic acid [9]. The life cycle assessment (LCA) of bio-adipic acid derived from these series

of processes revealed a reduction of 62–78% in the carbon dioxide emissions compared with the adipic acid derived from fossil fuels [10].

Concerning the catalytic hydrogenation of muconic acid, several studies have been conducted to identify the most effective catalyst capable of performing effectively even under mild conditions (e.g., low temperature and pressure). The most commonly used catalysts employed for this reaction are based on platinum group metals, in particular palladium (Pd) [11]. However, these metals are known for their low stability and high cost [12]. A possible solution to these problems can be found by adding a second metal [13–15] or by varying the type of support, altering the Pd active phase's structure, hence affecting the catalytic performance of the catalyst [16].

Both routes were investigated in previous works by our research group. In particular, Pd-Au [13] and Pd-Rh [17] bimetallic systems were investigated and exhibited interesting results in the MA hydrogenation. Likewise, in Capelli et al. [18], the effect of the different supports was investigated.

In the present work, we investigated the first route, and Pd was coupled with two different non-noble transition metals, Ni and Zn. The goal was to find suitable, high performance and cheaper catalysts able to guarantee a good catalytic activity and stability toward the hydrogenation of MA to bio-AdA. Nickel and zinc were chosen due to their high ability to interact with molecular hydrogen and to promote the hydrogenation of substrates, as well as their lower cost compared with palladium (26,011 USD/ton for Ni and 3006 USD/ton for Zn against the 65,000 USD/kg for Pd [19]). Indeed, by reducing the amount of palladium while retaining the same overall metal content, the inclusion of a second, less expensive metal can help to drastically lower the cost of the catalyst. Interesting results have already been reported on nickel-based catalysts for MA hydrogenation, although high hydrogen pressures and/or high metal loading have been used [20,21]. Zinc is commonly used as promoter for CO<sub>2</sub> hydrogenation to methanol [22]; moreover, several works have reported how unsaturated compounds, such as benzene and cinnamaldehyde, can be hydrogenated successfully using zinc-based catalysts [15,23–25]. Two bimetallic catalysts were synthesized with a total metal loading of 1%, in which the amount of Pd and Ni (or Zn) was indicated using subscripts in the label that indicate the molar ratio between Pd and the second metal. For example, Pd<sub>8</sub>Ni<sub>2</sub> means a catalyst with 1% of the total metal loading with a ratio between Pd and Ni equal to 8:2. The pre-formed nanoparticles were supported on high-temperature heat treated carbon nanofibers (HHT-CNFs), obtaining Pd<sub>8</sub>Ni<sub>2</sub>/HHT and Pd<sub>8</sub>Zn<sub>2</sub>/HHT. For both the catalysts, a sol-immobilization procedure was employed, as it allowed for obtaining a homogeneous distribution of the nanoparticles on the support, finely tuning the particle size, being performed at room temperature, and leading to low production costs [26]. All of the catalysts were characterized by transmission electron microscopy (TEM), inductively coupled plasma optical emission spectroscopy (ICP-OES), and X-ray photoelectron spectroscopy (XPS) analysis. They all showed satisfactory results characterized by a high conversion and selectivity with improved activity and stability when compared with monometallic palladium.

Regarding the muconic acid hydrogenation reaction, it was chosen to work with the sodium muconate salt. Indeed, although in a previous study it was found that *t,t*-MA hydrogenation was preferable to the Na-Muc molecule due to the higher reaction rate and AdA yield, using the first, there was not the possibility to increase substrate concentration above 1.42E-02 M, due to solubility limitations [27]. In addition to this, after the first fermentation process of biomass muconic acid (MA) was mainly in its *cis,cis*-sodium muconate (Na-Muc) form due to the alkalinity of the fermentation broth [8]. Because of these reasons, it was decided to work with this starting material to get as close as possible to the post-fermentation conditions of the biomass.

## 2. Results and Discussion

### 2.1. Hydrogenation Reaction

Two different catalysts were synthesized by the sol immobilization method and supported on high-temperature, heat-treated carbon nanofibers (HHT-CNFs). Indeed, it has been reported that the utilization of these supports can improve the catalytic activity of supported Pd nanoparticles compared with other carbonaceous supports [28]. The two synthesized catalysts (1%Pd<sub>8</sub>Ni<sub>2</sub>/HHT and 1%Pd<sub>8</sub>Zn<sub>2</sub>/HHT) were tested in the muconic acid hydrogenation reaction performed in a batch reactor and compared with the behavior of the monometallic one (1%Pd/HHT). The latter was previously synthesized for another work and already tested in different conditions [13].

The substrate conversion and the product yield were computed using Equations (1) and (3), respectively, and monitored via sampling after 15, 30, 60, 90, 120, and 180 min.

Already after 15 min of the reaction, the synthesized catalysts exhibited a greater MA conversion than the monometallic Pd (52%), namely 56% and 67% for Pd<sub>8</sub>Ni<sub>2</sub>/HHT and Pd<sub>8</sub>Zn<sub>2</sub>/HHT, respectively (Table 1, column 1).

**Table 1.** Summary of the catalytic results. Reaction conditions: MA concentration 0.1 M, temperature 70 °C, 2 bar pressure of H<sub>2</sub>, metal/substrate ratio 1/500.

Catalysts	MA Conversion after 15 min (%)	MA Conversion after 30 min (%)	AdA Yield after 3 h (%)
Pd/HHT	52	95	68
Pd <sub>8</sub> Ni <sub>2</sub> /HHT	56	100	80
Pd <sub>8</sub> Zn <sub>2</sub> /HHT	67	100	84

Full conversion of the substrate was obtained after 30 min for both the novel catalysts in contrast with monometallic palladium, which reached only 95% of conversion (Table 1, column 2). Comparing the results obtained with Pd<sub>8</sub>Ni<sub>2</sub>/HHT, it is possible to observe that the substrate was completely converted at a substantially lower pressure, metal percentage, and metal/substrate molar ratio than what was already reported in the literature [20].

Starting from *cis,cis*-sodium muconate, adipic acid was obtained with a yield higher than 80% after 3 h with both catalysts, specifically 80% and 84% for Pd<sub>8</sub>Ni<sub>2</sub>/HHT and Pd<sub>8</sub>Zn<sub>2</sub>/HHT, respectively. In contrast, the monometallic palladium catalyst reached only a yield of 68% at the same conditions (Table 1, column 3). In Figure 1, it is possible to appreciate the trend of AdA yield over the reaction pathway for the three catalysts compared. As mentioned before, the two synthesized catalysts showed a higher yield than monometallic Pd throughout the course of the reaction. The trend was then characterized by the presence of a plateau after 2 h of the reaction, which was more evident in the case of Pd<sub>8</sub>Zn<sub>2</sub>/HHT than in Pd<sub>8</sub>Ni<sub>2</sub>/HHT.

To investigate the catalyst performance, the initial activity after 15 min was evaluated using Equation (4). Pd<sub>8</sub>Ni<sub>2</sub> and Pd<sub>8</sub>Zn<sub>2</sub> bimetallic catalysts exhibited a higher initial activity (1108 h<sup>-1</sup> and 1199 h<sup>-1</sup>, respectively) than the monometallic Pd one (1066 h<sup>-1</sup>). This behavior confirms that the introduction of a second metal to Pd positively affected not only the conversion and the yield, but also the catalytic activity.

In terms of product selectivity, the reaction first occurred with the conversion of MA to three different mono-hydrogenated intermediates. This is the faster step of the reaction. Consequently, the intermediates were converted to AdA (Figure 2). This last step is the rate determining step of the reaction [29].

The selectivity after 15 min of reaction for every intermediate was calculated using Equation (3). The formation of the reaction intermediate followed the trend of initial activity calculated above. The most active catalyst, Pd<sub>8</sub>Zn<sub>2</sub>, showed a greater selectivity after 15 min towards 2Z-HyMA, with 37%, followed by Pd<sub>8</sub>Ni<sub>2</sub>, with 32%, and sequentially by monometallic Pd, with 28% (Figure 3). The results show that the intermediate was the most present for every reaction, succeeded by 2E-HyMA and 3E-HyMA, nevertheless the

starting *cis,cis* form. This behavior was desired because, regarding the reaction mechanism, 2*Z*-HyMA was quickly transformed to AdA compared with the other reactions. Indeed, the selectivity for the latter, 3*E*-HyMA, had the same results for each catalyst.

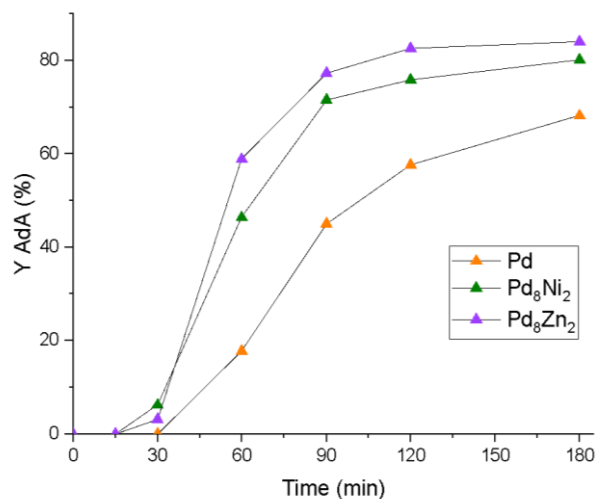


**Figure 1.** AdA production over the time for each of the catalysts. Reaction conditions: MA concentration 0.1 M, temperature 70 °C, 2 bar pressure of H<sub>2</sub>, metal/substrate ratio 1/500.

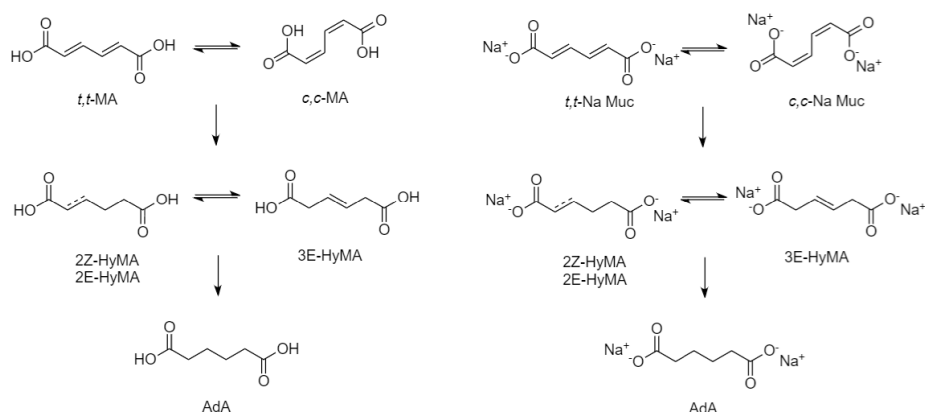


**Figure 2.** Scheme of MA (left) and Na-muconate (right) conversion to AdA.

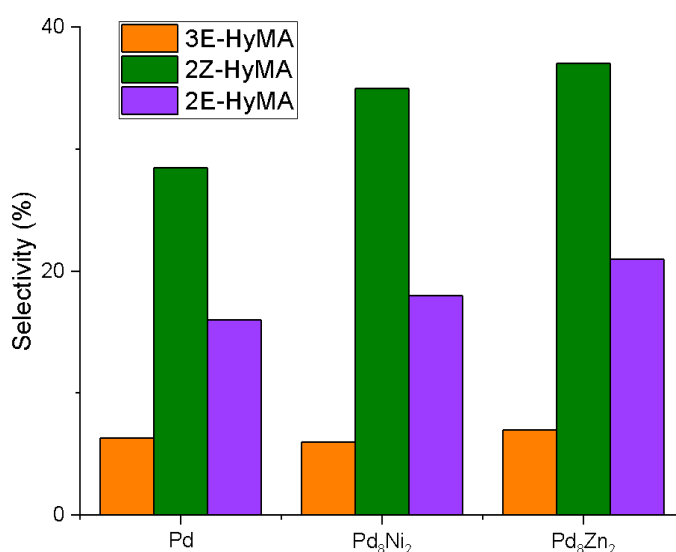


**Figure 3.** Intermediate selectivity after 15 min of reaction. Reaction conditions: MA concentration 0.1 M, temperature 70 °C, 2 bar pressure of H<sub>2</sub>, metal/substrate ratio 1/500.

Finally, to study the catalyst stability, recycling tests were performed by recovering the catalyst and running up to five repeated reactions. Every reaction was carried out for 2 h, after which the solid catalyst was recovered by filtration and, without washing, fed back into the reactor to be reused in the next reaction. As expected, monometallic Pd, underwent degradation from the third run onwards (Figure 4). Differently,  $\text{Pd}_8\text{Ni}_2$  and  $\text{Pd}_8\text{Zn}_2$  catalysts maintained 100% of MA conversion for up to five consecutive reactions (Figure 4, left).

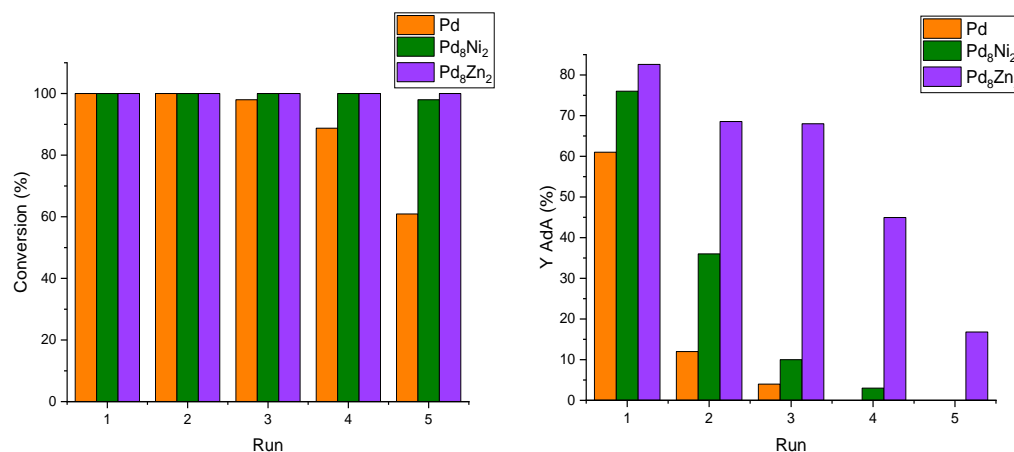


**Figure 4.** MA conversion (left) and yield of AdA (right) after 120 min during recycling tests.

Regarding adipic acid production, however, only  $\text{Pd}_8\text{Zn}_2$  continued to produce AdA up to five runs (Figure 4, right). Nonetheless, the  $\text{Pd}_8\text{Zn}_2$  catalyst showed a slight deactivation during the stability tests, probably due to metal leaching, as in the case of Pd. Therefore, even in this case, the presence of bimetallic NPs allowed for the synthesis of a more stable and active catalyst.

To evaluate the catalytic behavior of the studied catalysts in further detail, the hydrogenation reaction was conducted, changing the most important operative parameters, i.e., pressure, temperature, and substrate concentration. For this study, the catalyst that previously showed increased catalytic activity, namely  $1\%\text{Pd}_8\text{Zn}_2/\text{HHT}$ , was examined. Particular attention was paid to the effect of pressure on the catalytic activity of this catalyst, varying the pressure from 2 bar to 3 bar and 4 bar. The catalyst was also tested at various temperatures, 50 °C, 70 °C, and 90 °C. Additionally, the effect of the substrate concentration was investigated, and different concentrations of the substrate solution were utilized: 0.04 M, 0.08 M, and 0.1 M. These reactions were conducted for 1.5 h with a constant metal/substrate molar ratio of 1/500.

As expected, as the hydrogen pressure increased, the yield of adipic increased, reaching 90% after 1.5 h at 4 bar. In addition, full conversion of the initial substrate was reached within 15 min (Table 2).

**Table 2.** Summary of the catalytic results at different  $\text{H}_2$  pressures. Reaction conditions: MA concentration 0.1 M, temperature 70 °C, metal/substrate ratio 1/500, catalyst  $1\%\text{Pd}_8\text{Zn}_2/\text{HHT}$ .

Reaction Condition		MA Conversion after 15 min (%)	AdA Yield after 1.5 h (%)
H <sub>2</sub> Pressure	2 bar	67	77
	3 bar	100	85
	4 bar	100	90

Furthermore, in the instance of the study conducted at different temperatures, the adipic yield increased linearly as the temperature rose. The same held true for the conversion of the substrate, which achieved 100% after 15 min only at 90 °C. However, complete conversion was achieved after 30 min at all operating temperatures (Table 3).

**Table 3.** Summary of the catalytic results at different temperatures. Reaction conditions: MA concentration 0.1 M, 2 bar pressure of H<sub>2</sub>, metal/substrate ratio 1/500, catalyst 1%Pd<sub>8</sub>Zn<sub>2</sub>/HHT.

Reaction Condition		MA Conversion after 15 min (%)	AdA Yield after 1.5 h (%)
Temperature	50 °C	60	68
	70 °C	67	77
	90 °C	100	85

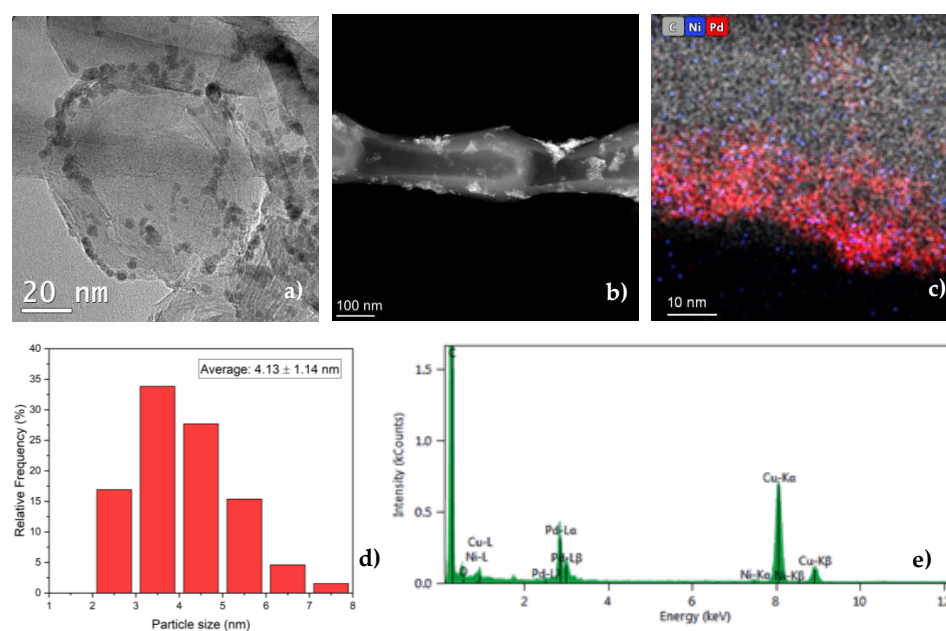
The production of adipic acid likewise increased with the increased substrate concentration. In this instance, however, a lower starting MA concentration favored the first equilibrium, resulting in a larger substrate conversion in the first 15 min of the reaction (Table 4). The reaction then proceeded regularly, with the complete substrate conversion occurring after 30 min at all operating conditions and the final adipic acid yield increasing as the MA concentration rose.

**Table 4.** Summary of the catalytic results at different substrate concentrations. Reaction conditions: temperature 70 °C, 2 bar pressure of H<sub>2</sub>, metal/substrate ratio 1/500, catalyst 1%Pd<sub>8</sub>Zn<sub>2</sub>/HHT.

Reaction Condition		MA Conversion after 15 min (%)	AdA Yield after 1.5 h (%)
MA concentration	0.04 M	97	20
	0.08 M	95	65
	0.1 M	67	77

## 2.2. Characterization

The catalysts' morphology, particle size distribution, and metals ratio were evaluated by TEM and HAADF-STEM analyses. The bimetallic catalysts showed an average particle size of  $4.1 \pm 1.1$  nm and  $4.3 \pm 0.9$  nm, respectively, for Pd<sub>8</sub>Ni<sub>2</sub> (Figure 5a,b) and Pd<sub>8</sub>Zn<sub>2</sub> (Figure 6a,b), with a narrow particle size distribution. These values were in agreement with what was usually obtained with the sol immobilization technique and they were comparable with the value of  $3.9 \pm 1.2$  nm obtained from the analysis previously made on Pd/HHT [13].

**Figure 5.** (a) TEM, (b) HAADF-STEM, (c–e) XEDS mapping and spectrum of a representative area, and (d) particle size distribution of 1%Pd<sub>8</sub>Ni<sub>2</sub>/HHT.

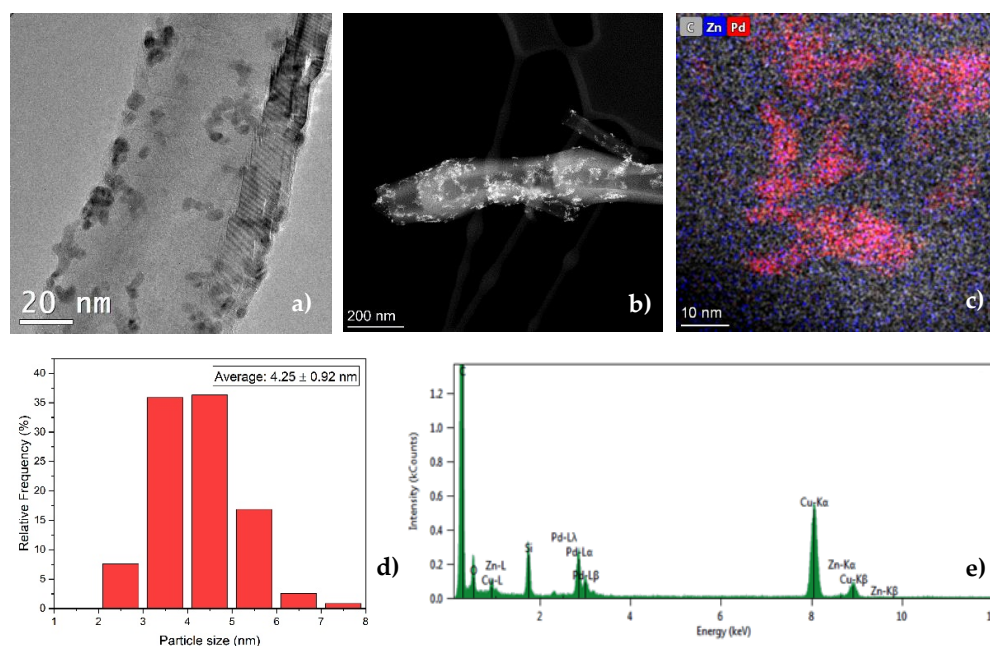


**Figure 6.** (a) TEM, (b) HAADF-STEM, (c–e) XEDS mapping and spectrum of a representative area, and (d) particle size distribution of 1%Pd<sub>8</sub>Zn<sub>2</sub>/HHT.

By using STEM-XEDS analysis, the amounts of Pd and Ni/Zn for the two different catalysts were evaluated. The calculated values were lower than the nominal ones (Table 5). This behavior could be explained by the presence of segregation or non-immobilization of the metals. However, the STEM-XEDS images allowed for confirming the presence of the Ni and Zn, also highlighting a prevalence of the atoms of the second metal close to those of Pd.

**Table 5.** Nominal and calculated metal molar ratio for the synthesized catalysts.

Catalysts	Nominal Pd-X Molar Ratio	Calculated Pd-X Molar Ratio (TEM-XEDS)	Calculated Pd-X Molar Ratio (ICP)
Pd <sub>8</sub> Ni <sub>2</sub> /HHT	80-20	96-4	96-4
Pd <sub>8</sub> Zn <sub>2</sub> /HHT	80-20	94-6	93-7

To deepen the divergence between the nominal and calculated atomic ratio, inductively coupled plasma optical emission spectroscopy (ICP-OES) analyses were performed on the two catalysts. The results obtained revealed a lower metal loading compared with the nominal ones, specifically for the second metal, which never exceeded 10% (Table 5). These results allowed for exclude the segregation of bimetallic NPs, supporting the hypothesis of the partial non-immobilization of the second metal on the support during the synthesis.

Inductively coupled plasma optical emission spectroscopy (ICP-OES) was also performed on the catalysts used in the recycling tests. In Table 6, the percentages of each metal are reported, the values are related to the total amount of solid catalyst. This analysis allowed for confirming deactivation due to leaching of the metals with an average loss of 30-40% for all of the bimetallic catalysts. In particular, Pd leaching for both catalysts could be clearly seen. Whereas, Ni and Zn contents were the same both before and after the recycling tests.

X-ray photoelectron spectroscopy (XPS) was employed to obtain information on the surface properties of the catalysts (Table 7). From the XPS survey spectra, only C 1s (284.4–284.6 eV), O 1s (532.6–533.4 eV), and Pd 3d (335.7–337.6 eV) could be detected. Both Ni and Zn were not detected by the analysis. An explanation for these results can be found in the low amount of the two metals, detected by previous analyses, under the limit of detection of the instrument used for these analyses.

**Table 6.** Results of inductively coupled plasma optical emission spectroscopy (ICP-OES) analyses on fresh and used catalysts. The percentages of metals are related to the total amount of solid catalyst.

	Pd (%)	Ni (%)	Zn (%)
Pd <sub>8</sub> Ni <sub>2</sub> /HHT fresh	0.92	0.04	-
Pd <sub>8</sub> Ni <sub>2</sub> /HHT used	0.53	0.04	-
Pd <sub>8</sub> Zn <sub>2</sub> /HHT fresh	0.93	-	0.07
Pd <sub>8</sub> Zn <sub>2</sub> /HHT used	0.62	-	0.09

**Table 7.** Results of the XPS survey spectra.

		C 1s	O 1s	Pd 3d
Pd/HHT	B.E. (eV)	284.6	532.6	337.6
	% At.	92.12	7.24	0.57
Pd <sub>8</sub> Ni <sub>2</sub> /HHT	B.E. (eV)	284.6	533.2	335.7
	% At.	93.39	6.32	0.29
Pd <sub>8</sub> Zn <sub>2</sub> /HHT	B.E. (eV)	284.4	533.4	335.7
	% At.	96.13	3.40	0.47

From a detailed high-resolution (HR) analysis of the Pd 3d region, and in particular of the metallic palladium contribution (Pd0), a lower BE shift of  $-0.70$  and  $-0.65$  eV was observed for Pd<sub>8</sub>Ni<sub>2</sub>/HHT and Pd<sub>8</sub>Zn<sub>2</sub>/HHT, respectively (Table 8). This modification underlined an electron donation from the second metal (Ni or Zn) to Pd, and in fact a lower BE is synonymous with an electronic density donation, as it has been shown in reference [30].

**Table 8.** Results of the HR spectra for the Pd 3d regions.

		Pd(0)	Shift Pd(0)
Pd/HHT	B.E. (eV)	336.4	-
Pd <sub>8</sub> Ni <sub>2</sub> /HHT	B.E. (eV)	335.70	$-0.70$
Pd <sub>8</sub> Zn <sub>2</sub> /HHT	B.E. (eV)	335.75	$-0.65$

### 3. Materials and Methods

#### 3.1. Materials and Chemicals

Sodium tetrachloropalladate (II) (Na<sub>2</sub>PdCl<sub>4</sub>, 99.99%), nickel chloride (NiCl<sub>2</sub>\*6H<sub>2</sub>O, 99.99%), zinc chloride (ZnCl<sub>2</sub>, 99.99%), sodium borohydride (NaBH<sub>4</sub>, 99.99%), and polyvinyl alcohol (PVA, average molar weight 10000, 87–89% hydrolyzed) were purchased from Merck (Haverhill, MA, USA) and were used without any pre-treatment. All of the catalytic tests were carried out using cis,cis-muconic acid (Merck,  $\geq 97\%$ ) and deionized water as the substrate and the solvent, respectively. To salsify the muconic acid, sodium hydroxide (Merck,  $\geq 97\%$ ) was used. CNFs PR24-HHT (high heat-treated carbon nanofiber), used as support, were obtained from the Applied Science Company (Cedarville, OH, USA).

#### 3.2. Catalysts Synthesis

All of the catalysts, as well as Pd/HHT [13], were synthesized using the sol immobilization technique. The following procedure was employed for 1 g of 1 wt% bimetallic catalyst (Pd<sub>8</sub>Ni<sub>2</sub> and Pd<sub>8</sub>Zn<sub>2</sub>) supported on high heat-treated carbon nano fiber (HHT-CNFs).

The whole process was conducted in an inert atmosphere (nitrogen) in order to avoid Ni and Zn oxidation. Indeed, milliQ water was previously degassed in a vacuum for 1 h and then purged in N<sub>2</sub> for 30 min.

For every catalyst, the proper amount of precursor salts (K<sub>2</sub>PdCl<sub>4</sub>, ZnCl<sub>2</sub>, NiCl<sub>2</sub>\*6H<sub>2</sub>O) (Table 9) was added into a baker containing 400 mL of milliQ water. Then, the stabilizing agent PVA (Metal/PVA = 1/0.65 (wt/wt)) was inserted. After 3 min, the appropriate

amount of freshly prepared aqueous solution of NaBH<sub>4</sub> ( $M/\text{NaBH}_4 = 1/8$  (mol/mol)) was added to the mixture at once and the instantaneous formation of metallic colloid was proven by the change in color of the solution. After that, under vigorous stirring, the colloidal solution was added to the support, previously dispersed in degassed water, in order to anchor the NPs to the support. Through the addition of sulfuric acid (H<sub>2</sub>SO<sub>4</sub>), the suspension was acidified until pH 2 and stirred for 2 h to guarantee the total immobilization of NPs on the selected support [21]. The solid was then filtered, washed with 1 L of deionized water, and dried in an oven at 80 °C for 48 h to obtain the final catalytic materials.

**Table 9.** Summary of the amount of the metals for the preparation of the sol.

Catalysts	Pd [mmol × 10 <sup>-2</sup> ]	Ni [mmol × 10 <sup>-2</sup> ]	Zn [mmol × 10 <sup>-2</sup> ]
Pd/HHT	9.40	-	-
Pd <sub>8</sub> Ni <sub>2</sub> /HHT	8.26	2.06	-
Pd <sub>8</sub> Zn <sub>2</sub> /HHT	8.15	-	2.04

### 3.3. Hydrogenation Reaction

The hydrogenation reactions were carried out in a batch glass reactor placed in an oil bath equipped with a magnetic stirrer and a thermocouple to control the temperature. Before every reaction, the catalyst was regenerated with hydrogen.

All of the reactions were carried out at 70 °C and the reactor was pressurized at 2 bar absolute of hydrogen. The reactions were performed with a metals/substrate molar ratio selected of 1/500 and at 1400 rpm, allowing to keep a kinetic regime. Typically, 25 mL of a 0.1 M demineralized water solution of Na-muconate was prepared by adding 355.5 mg (2.5 mmol) of cis,cis-muconic acid and 2 equivalents (5.0 mmol) of NaOH and then sonicating until the solid was completely dissolved. Litmus paper was used to measure the pH of the solution after the solids had completely dissolved to ensure that it was within the proper pH range and that there was no extra base. The solution was placed in the reactor and the reaction was started.

The reaction was monitored by sampling after 15, 30, 60, 90, 120, and 180 min, after quenching the reaction in the sample vials. The reaction products were analyzed with high-performance liquid chromatography (HPLC) equipped with an ultra-visible (UV) detector set at 210 nm and a Rezex ROA-Organic Acid H<sup>+</sup> (8%) column. The solvent was 0.005 M H<sub>2</sub>SO<sub>4</sub>. The column temperature was set at 60 °C. The flow rate was 0.6 mL/min. With this set up, all the intermediates, the substrate, and AdA were separated. Because of the unavailability of commercial standards of the intermediates, these products were identified in our previous work by <sup>1</sup>H-NMR analysis [11]. This allowed us to monitor the MA conversion and the selectivity towards the intermediates and the product.

Recycle tests were carried out with the same setup used for the hydrogenation reaction. The reactor was filled with 25 mL of 0.1 M demineralized water solution of Na-muconate and catalysts and then pressurized at 2 bar of hydrogen. The hydrogenation reaction was conducted at 70 °C under stirring at 1400 rpm for 120 min. After this time, a liquid sample of the reaction mixture was analyzed with HPLC/UV to evaluate conversion. The catalyst was then filtered and reused for the next run. With this procedure, it was possible to evaluate MA conversion for five consecutive cycles.

The MA conversion was evaluated using Equation (1)

$$\text{Conversion (\%)} = \frac{\text{mol}_{IN} - \text{mol}_{OUT}}{\text{mol}_{IN}} \cdot 100 \quad (1)$$

where  $\text{mol}_{IN}$  are the moles of the substrate initially used for the reaction, while  $\text{mol}_{OUT}$  are the moles of the substrate that remain after the reaction.

The selectivity and product yield were evaluated using Equations (2) and (3), respectively.

$$\text{Selectivity}_n (\%) = \frac{\text{mol}_n}{\text{mol}_n + \sum \text{mol}_i} \cdot 100 \quad (2)$$

where  $mol_n$  is the number of moles of the considered reaction product and  $\Sigma mol_i$  is the sum of the moles of all the products.

$$Yield_n(\%) = \frac{Selectivity_n(\%)}{100} \cdot Conversion(\%) \quad (3)$$

Initial activity after 15 min of reaction was also evaluated considering the MA reacted moles (after 15 min) and the total metal amount used for the reaction (Equation (4)).

$$Initial\ activity\ (h^{-1}) = \frac{mol_{MA\ reacted}}{mol_{met} \cdot reaction\ time\ (h)} \quad (4)$$

### 3.4. Catalysts Characterization

The morphology and microstructures of the catalysts were characterized by transmission electron microscopy (TEM) using a FEI Tecnai F20 Field Emission Gun (FEG) microscope, working at an accelerating voltage of 200 kV. The average particle diameter ( $d$ ) was estimated using the following expression:  $d = \Sigma n_i d_i / \Sigma n_i$ , where  $n_i \geq 200$ . The total metal dispersion was computed according to  $D = N_s / N_t$ , where  $N_s$  is the total number of surface-metal atoms and  $N_t$  is the total number of atoms in the metal particle. For the particle size calculations, ImageJ software was used.

The metal particle composition was evaluated using a high-angle annular dark-field (HAADF) scanning transmission electron microscopy (STEM) and energy-dispersive X-ray spectroscopy (EDX). To perform these analyses a TEM/STEM FEI Talos F200X G20 microscope, equipped with 4 Super-X SDDs, was employed.

Metal loading and metal leaching were evaluated by inductively coupled plasma optical emission spectroscopy (ICP-OES) using a Perking Elmer Optima 8000 emission. The analyses were performed on the solution obtained after the mineralization of the solid catalyst.

X-ray photoelectron spectroscopy (XPS) analyses were performed using a Thermo Fisher Scientific K-alpha+. The samples were analyzed using a monochromatic Al X-ray source operating at 72 W. All the data were recorded at 150 eV for survey scans and at 40 eV for high-resolution (HR) spectra with a 1 eV and 0.1 eV step size, respectively. The analyses of the data were executed using the CASAXPS (v2.3.17 PR1.1) program.

## 4. Conclusions

Two different bimetallic catalysts were synthesized and tested in the muconic acid hydrogenation reaction to produce adipic acid. To enhance the activity and stability of the palladium catalyst often used for this reaction, it was decided to combine palladium with two metals of the first transition, namely nickel and zinc. Indeed, an additional objective was to lower the costs of the catalytic system for this reaction, with compared with what had been previously published, by decreasing the amount of palladium and replacing it with a less expensive metal, while maintaining the same catalytic performances. The catalysts synthesized were  $Pd_8Ni_2$  and  $Pd_8Zn_2$ , with a metal loading of 1% and supported on HHT-CNFs. All of the catalysts exhibited enhanced catalytic performances with respect to monometallic palladium in terms of conversion, catalytic activity, and selectivity. Different reaction conditions were investigated to study the influence of pressure, temperature, and substrate concentration. The yield of adipic acid at the end of the process increased by increasing the hydrogen pressure in the head space of the reactor, the temperature, and the initial concentration of the substrate. The catalysts were characterized using TEM and STEM-XEDS analysis, ICP, and XPS. TEM characterizations showed an average particle size of about 4 nm for both synthesized catalysts, with a narrow particle size distribution. STEM-XEDS and ICP analyses showed a calculated metal molar ratio lower than the nominal ones, with respect to the second metal. This behavior can be explained by the partial non-immobilization of the second metal on the support during the synthesis. Despite this, XPS analysis showed a shift of the Pd 3d peak values, indicating an electronic

exchange from the second metal (Ni or Zn) to Pd that enhanced the catalytic activity of monometallic Pd. In conclusion, these results pointed out that even a small amount of these two metals, in particular Zn, enhanced the catalytic properties of monometallic Pd against the hydrogenation reaction of muconic acid. In particular, it allowed not only for an increase in the yield of production of adipic acid, but above all it influenced the stability of the catalyst in the reusability tests. Further studies will be aimed at optimizing the synthesis of these catalysts in order to improve their stability, in particular avoiding metal leaching.

**Author Contributions:** Conceptualization, E.Z., A.V. (Alberto Villa) and C.P.; methodology, E.Z., A.V. (Alberto Villa) and C.P.; software, E.Z., S.B. and A.V. (Alessandro Vomero); validation, E.Z., L.S. and C.P.; formal analysis, E.Z., A.V. (Alberto Villa), and C.P.; investigation, E.Z. and L.S.; resources, A.V. (Alberto Villa) and C.P.; data curation, E.Z., L.S., S.B. and A.V. (Alessandro Vomero); writing—original draft preparation, E.Z. and L.S.; writing—review and editing, all of the authors; visualization, all the authors; supervision, A.V. (Alberto Villa) and C.P.; project administration, A.V. (Alberto Villa) and C.P.; funding acquisition, A.V. (Alberto Villa) and C.P. All authors have read and agreed to the published version of the manuscript.

**Funding:** This research received no external funding.

**Data Availability Statement:** Please write to carlo.pirola@unimi.it for the research data availability.

**Acknowledgments:** The work was partially financed by the projects “Poliammidoammine: una nuova classe di ritardanti di fiamma polimerici per tessuti cellululosici” and “Photocarbon” in the calls “Piano di Sostegno alla Ricerca (PSR 2020 and 2021)” by Dipartimento di Chimica, Università degli Studi di Milano.

**Conflicts of Interest:** The authors declare no conflict of interest.

## References

1. Brundtland, G.H. Our Common Future—Call for Action. *Environ. Conserv.* **1987**, *14*, 291–294. [[CrossRef](#)]
2. Anastas, P.T.; Warner, J.C. Principles of Green Chemistry. *Green Chem. Theory Pract.* **1998**, 29–56.
3. Skoog, E.; Shin, J.H.; Saez-Jimenez, V.; Mapelli, V.; Olsson, L. Biobased Adipic Acid—The Challenge of Developing the Production Host. *Biotechnol. Adv.* **2018**, *36*, 2248–2263. [[CrossRef](#)] [[PubMed](#)]
4. Braga, M.; Ferreira, P.M.; Almeida, J.R.M. Screening Method to Prioritize Relevant Bio-based Acids and Their Biochemical Processes Using Recent Patent Information. *Biofuels Bioprod. Biorefin.* **2021**, *15*, 231–249. [[CrossRef](#)]
5. Thiemens, M.H.; Trogler, W.C. Nylon Production: An Unknown Source of Atmospheric Nitrous Oxide. *Science* **1991**, *251*, 932–934. [[CrossRef](#)]
6. Kruyer, N.S.; Peralta-Yahya, P. Metabolic Engineering Strategies to Bio-Adipic Acid Production. *Curr. Opin. Biotechnol.* **2017**, *45*, 136–143. [[CrossRef](#)]
7. Almqvist, H.; Veras, H.; Li, K.; Garcia Hidalgo, J.; Hultberg, C.; Gorwa-Grauslund, M.; Skorupa Parachin, N.; Carlquist, M. Muconic Acid Production Using Engineered Pseudomonas Putida KT2440 and a Guaiacol-Rich Fraction Derived from Kraft Lignin. *ACS Sustain. Chem. Eng.* **2021**, *9*, 8097–8106. [[CrossRef](#)]
8. Johnson, C.W.; Salvachúa, D.; Khanna, P.; Smith, H.; Peterson, D.J.; Beckham, G.T. Enhancing Muconic Acid Production from Glucose and Lignin-Derived Aromatic Compounds via Increased Protocatechuate Decarboxylase Activity. *Metab. Eng. Commun.* **2016**, *3*, 111–119. [[CrossRef](#)]
9. Draths, K.M.; Frost, J.W. Environmentally Compatible Synthesis of Adipic Acid from D-Glucose. *J. Am. Chem. Soc.* **1994**, *116*, 399–400. [[CrossRef](#)]
10. Corona, A.; Bidy, M.J.; Vardon, D.R.; Birkved, M.; Hauschild, M.Z.; Beckham, G.T. Life Cycle Assessment of Adipic Acid Production from Lignin. *Green Chem.* **2018**, *20*, 3857–3866. [[CrossRef](#)]
11. Vardon, D.R.; Rorrer, N.A.; Salvachúa, D.; Settle, A.E.; Johnson, C.W.; Menart, M.J.; Cleveland, N.S.; Ciesielski, P.N.; Steirer, K.X.; Dorgan, J.R. Cis, Cis-Muconic Acid: Separation and Catalysis to Bio-Adipic Acid for Nylon-6, 6 Polymerization. *Green Chem.* **2016**, *18*, 3397–3413. [[CrossRef](#)]
12. Dong, H.; Zhao, J.; Chen, J.; Wu, Y.; Li, B. Recovery of Platinum Group Metals from Spent Catalysts: A Review. *Int. J. Miner. Process.* **2015**, *145*, 108–113. [[CrossRef](#)]
13. Capelli, S.; Barlocco, I.; Scesa, F.M.; Huang, X.; Wang, D.; Tessore, F.; Villa, A.; Di Michele, A.; Pirola, C. Pd–Au Bimetallic Catalysts for the Hydrogenation of Muconic Acid to Bio-Adipic Acid. *Catalysts* **2021**, *11*, 1313. [[CrossRef](#)]
14. Li, L.; Gan, Y.-M.; Lu, Z.-H.; Yu, X.; Qing, S.; Gao, Z.; Zhang, R.; Feng, G. The Effects of Fe, Co and Ni Doping in CuAl<sub>2</sub>O<sub>4</sub> Spinel Surface and Bulk: A DFT Study. *Appl. Surf. Sci.* **2020**, *521*, 146478. [[CrossRef](#)]
15. Li, J.; Shi, L.; Feng, G.; Shi, Z.; Sun, C.; Kong, D. Selective Hydrogenation of Naphthalene over  $\gamma$ -Al<sub>2</sub>O<sub>3</sub>-Supported NiCu and NiZn Bimetal Catalysts. *Catalysts* **2020**, *10*, 1215. [[CrossRef](#)]

16. Liu, J.J. Advanced Electron Microscopy of Metal-Support Interactions in Supported Metal Catalysts. *ChemCatChem* **2011**, *3*, 934–948. [[CrossRef](#)]
17. Barlocco, I.; Capelli, S.; Zanella, E.; Chen, X.; Delgado, J.J.; Roldan, A.; Dimitratos, N.; Villa, A. Synthesis of Palladium-Rhodium Bimetallic Nanoparticles for Formic Acid Dehydrogenation. *J. Energy Chem.* **2021**, *52*, 301–309. [[CrossRef](#)]
18. Capelli, S.; Motta, D.; Evangelisti, C.; Dimitratos, N.; Prati, L.; Pirola, C.; Villa, A. Effect of Carbon Support, Capping Agent Amount, and Pd NPs Size for Bio-Adipic Acid Production from Muconic Acid and Sodium Muconate. *Nanomaterials* **2020**, *10*, 505. [[CrossRef](#)]
19. LME—London Metal Exchange. Available online: <https://www.lme.com/Market-data/LME-reference-prices/LME-Official-Price> (accessed on 30 November 2022).
20. Scelfo, S.; Pirone, R.; Russo, N. Highly Efficient Catalysts for the Synthesis of Adipic Acid from Cis,Cis-Muconic Acid. *Catal. Commun.* **2016**, *84*, 98–102. [[CrossRef](#)]
21. Matthiesen, J.E.; Carraher, J.M.; Vasiliu, M.; Dixon, D.A.; Tessonnier, J.-P. Electrochemical Conversion of Muconic Acid to Biobased Diacid Monomers. *ACS Sustain. Chem. Eng.* **2016**, *4*, 3575–3585. [[CrossRef](#)]
22. Allam, D.; Bennici, S.; Limousy, L.; Hocine, S. Improved Cu- and Zn-Based Catalysts for CO<sub>2</sub> Hydrogenation to Methanol. *Comptes Rendus Chim.* **2019**, *22*, 227–237. [[CrossRef](#)]
23. Hu, S.-C.; Chen, Y.-W. Partial Hydrogenation of Benzene on Ru–Zn/SiO<sub>2</sub> Catalysts. *Ind. Eng. Chem. Res.* **2001**, *40*, 6099–6104. [[CrossRef](#)]
24. Marchi, A.J.; Gordo, D.A.; Trasarti, A.F.; Apesteguía, C.R. Liquid Phase Hydrogenation of Cinnamaldehyde on Cu-Based Catalysts. *Appl. Catal. A Gen.* **2003**, *249*, 53–67. [[CrossRef](#)]
25. Mahata, N.; Gonçalves, F.; Pereira, M.F.R.; Figueiredo, J.L. Selective Hydrogenation of Cinnamaldehyde to Cinnamyl Alcohol over Mesoporous Carbon Supported Fe and Zn Promoted Pt Catalyst. *Appl. Catal. A Gen.* **2008**, *339*, 159–168. [[CrossRef](#)]
26. Prati, L.; Villa, A. The Art of Manufacturing Gold Catalysts. *Catalysts* **2011**, *2*, 24–37. [[CrossRef](#)]
27. Capelli, S.; Motta, D.; Evangelisti, C.; Dimitratos, N.; Prati, L.; Pirola, C.; Villa, A. Bio Adipic Acid Production from Sodium Muconate and Muconic Acid: A Comparison of Two Systems. *ChemCatChem* **2019**, *11*, 3075–3084. [[CrossRef](#)]
28. Sanchez, F.; Alotaibi, M.H.; Motta, D.; Chan-Thaw, C.E.; Rakotomahevitra, A.; Tabanelli, T.; Roldan, A.; Hammond, C.; He, Q.; Davies, T.; et al. Hydrogen Production from Formic Acid Decomposition in the Liquid Phase Using Pd Nanoparticles Supported on CNFs with Different Surface Properties. *Sustain. Energy Fuels* **2018**, *2*, 2705–2716. [[CrossRef](#)]
29. Rosengart, A.; Pirola, C.; Capelli, S. Hydrogenation of Trans, Trans-Muconic Acid to Bio-Adipic Acid: Mechanism Identification and Kinetic Modelling. *Processes* **2020**, *8*, 929. [[CrossRef](#)]
30. Xin, H.; Vojvodic, A.; Voss, J.; Nørskov, J.K.; Abild-Pedersen, F. Effects of D-Band Shape on the Surface Reactivity of Transition-Metal Alloys. *Phys. Rev. B* **2014**, *89*, 115114. [[CrossRef](#)]

**Disclaimer/Publisher’s Note:** The statements, opinions and data contained in all publications are solely those of the individual author(s) and contributor(s) and not of MDPI and/or the editor(s). MDPI and/or the editor(s) disclaim responsibility for any injury to people or property resulting from any ideas, methods, instructions or products referred to in the content.